# Line analysis of EUV Spectra from Molybdenum and Tungsten Injected with Impurity Pellets in LHD

Malay Bikas CHOWDHURI, Shigeru MORITA[1], Motoshi GOTO[1],
Hiroaki NISHIMURA[2], Keiji NAGAI  and Shinsuke FUJIOKA[2]

*Department of Fusion Science, Graduate University for Advanced Studies,*
*Toki 509-5292, Japan*
*[1]National Institute for Fusion Science, Toki 509-5292, Japan*
*[2]Institute of Laser Engineering, Osaka University, Suita 565-0871, Japan*

Spectroscopic data on high-Z materials for impurity diagnostics are important due to its possible use as a plasma facing component in the next generation fusion device. For this purpose molybdenum and tungsten are injected by an impurity pellet injector into the large helical device (LHD) plasmas. Emissions from such highly ionized elements mostly fall in extreme ultraviolet (EUV) and soft X-ray ranges. The EUV spectra in a range of 20-500 Å are recorded using a flat-field EUV spectrometer. The observed emissions are identified with the help of its temporal evolution and detailed analysis is done with electron temperature profiles. At high central electron temperature (~2.2 keV) molybdenum appears as an Al-, Mg- and Na-like ionization stages. Typical examples of identified transitions are Mo XXXI 190.46 Å ($3s^2$ $^1$S-3s3p $^3$P) and Mo XXXII 176.63 Å (3s $^2$S-3p $^2$P). For tungsten, on the other hand, three well-separated bands appear in wavelength range of 24-80 Å. The transitions around 33 Å have been tentatively identified with the help of calculated values. Most of the isolated lines on the top of pseudo-continuum bands around 50 and 60 Å are identified, and the wavelengths are compared with previous experimental studies and also with calculated values.

## 1. Introduction

Next generation fusion device will produce further heat load onto the first wall and divertor plates, and it may give rise to a serious damage to such plasma facing components. It is widely known that the high-Z materials instead of carbon become favorable to the plasma facing material, because such materials have less sputtering yield in addition to their high melting point [1]. At present, the use of tungsten [2] and molybdenum [3] is planned in ITER as a candidate for the divertor material. Then, the spectroscopic study on the high-Z impurities becomes important in the next generation fusion device. The spectral lines of the high-Z elements, however, have not been well investigated until now, e.g., even their wavelengths. Most of the spectral lines from the high-Z elements are at least emitted in extreme ultraviolet (EUV) and soft X-ray ranges when the electron temperature is greater than 1-2 keV. An extensive study is necessary on the line analysis of the high-Z elements in addition to a theoretical work on atomic physics.

For this purpose molybdenum and tungsten have been injected in large helical device (LHD) plasmas using an impurity pellet injector [4]. The emission spectra have been monitored with a flat-field EUV spectrometer [5] to iden-

tify their wavelengths and to analyze their time behaviors as a function of electron temperature. In this paper results on possible identification of the spectral lines emitted from highly ionized tungsten and molybdenum are presented with EUV spectra in wavelength range of 20-500 Å. The wavelengths of spectral lines identified here are also compared with previous experimental and calculated values.

## 2. Experimental Setup

Data are recorded from LHD discharges with magnetic field strength of 2.64 T and average plasma major and minor radii of 3.75 m and 60 cm, respectively. Three tangential negative-ion-based neutral beam injection (NBI) devices were used to initiate and heat the plasma up to an electron temperature ($T_e$) of 2.5 keV. Line-average electron densities were in the range of $1\text{-}4 \times 10^{13}$ cm$^{-3}$. Cylindrical carbon impurity pellets involving thin tungsten and molybdenum wires [6] have been injected perpendicularly to the toroidal plasma axis at the equatorial plane. The pellet size used in the present experiment was 0.8 mm in diameter and 0.8 mm in length and the wire size was 0.2 mm in diameter and 0.5 mm in length. The EUV emission spectra from the injected materials were measured by a flat-field EUV spectrometer with a 1200 lines/mm laminar-type holographic

grating. The distance between the grating center and the entrance slit is 237 mm and the distance between the focal plane perpendicular to the grating surface and the grating center is 235 mm. A back-illuminated vacuum ultra-violet (VUV) sensitive charge coupled device (CCD) detector was mounted at the focal position. The size of the CCD is 26.6×6.6 mm$^2$ with a pixel size of 26×26 μm$^2$ and the number of channels of 1024×255. The CCD detector was cooled down to −20°C to suppress the thermal noise and operated in 'full-binning mode' to take the signal output with a time interval of 5 ms. The spectral resolution of the spectrometer is 0.16 Å at 70 Å. The first and higher order emissions from C VI and other intrinsic impurity lines were used as a marker for the wavelength calibration. The whole spectra (20-500 Å) were recorded from several discharges by moving the CCD detector since the spectrometer can measure only a wavelength interval of 160 Å at a time. The charge states of measured lines are mainly determined by temporal variations of the line intensities after the pellet injection and during temperature decay phase at the end of discharges.

# 3. EUV Spectra and Analysis
## 3.1 Molybdenum

Figure 1 revealed the EUV spectrum from highly ionized molybdenum in the wavelength range of 20-165 Å. The last 25 Å between 140 and 165 Å was composed of another similar discharge. The highest ionization state of Na-like Mo (Mo XXXII; I.E.-1719.32 eV) has been observed in this experiment where the central electron temperature was 2.5 keV at the pellet injection. The central electron temperature rapidly drops to nearly 1.8 keV after the impurity pellet injection and recovered to 2.2 keV with decrease in the electron density. The Mo emissions begin to appear at 25 ms after the pellet injection and are continuously observable during the following 500 ms. A complicated structure is seen at 65-90 Å. This unresolved spectral array mostly consists of charge stages of Mo XXIV-Mo XXVIII, but the precise identification is now impossible. These charge states belong to K-like through P-like molybdenum ions and the lines therefore mainly have tran-
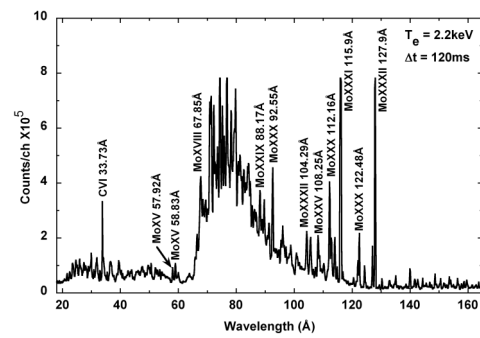


Fig. 1   Mo spectrum in 20-165 Å.

Table 1 Observed transitions of Mo ions in 65-90 Å.

| Ionization stages | Transitions | Wavelengths (Å) | | | |
|---|---|---|---|---|---|
| | | Present experiment | Previous experiment | Calculated | Predicted |
| MoXXIV | $3p^63d\ ^2D_{3/2}-3p^53d^2(^3F)\ ^2D_{3/2}$ | 70.83±0.02 | 70.8 [ 9] | 68.9 [10] | |
| | $3p^63d\ ^2D_{5/2}-3p^53d^2(^3P)\ ^2P_{3/2}$ | 71.34±0.03 | 71.24 [ 9] | 70.1 [10] | |
| | $3p^63d\ ^2D_{5/2}-3p^53d^2(^3F)\ ^2D_{5/2}$ | 72.22±0.02 | 72.12 [ 9] | 70.2 [10] | |
| | $3p^63d\ ^2D_{3/2}-3p^53d^2(^1S)\ ^2P_{1/2}$ | 73.50±0.05 | 73.300 [ 8] | | |
| | $3p^63d\ ^2D_{5/2}-3p^53d^2(^3F)\ ^2F_{7/2}$ | 75.17±0.02 | 75.0 [10] | 74.1 [10] | |
| | $3p^63d\ ^2D_{3/2}-3p^53d^2(^3F)\ ^2F_{5/2}$ | 77.38±0.05 | 77.354 [ 8] | | |
| MoXXV | $3p^6\ ^1S_0-3p^53d\ ^1P_1$ | 74.40±0.02 | 74.2 [ 9] | 73.1 [10] | |
| MoXXVI | $3p^5\ ^2P_{3/2}-3p^4(^1D)3d\ ^2P_{1/2}$ | 72.61±0.04 | 72.7 [10] | 69.5 [10] | |
| | $3p^5\ ^2P_{3/2}-3p^4(^3P)3d\ ^2P_{3/2}$ | 75.82±0.06 | 75.2 [10] | 72.8 [10] | |
| | $3p^5\ ^2P_{3/2}-3p^4(^3P)3d\ ^2D_{5/2}$ | 76.85±0.05 | 76.73 [ 9] | 73.4 [10] | |
| | $3p^5\ ^2P_{3/2}-3p^4(^1D)3d\ ^2S_{1/2}$ | 78.16±0.05 | 78.4 [10] | 75.7 [10] | |
| | $3p^5\ ^2P_{3/2}-3p^4(^1S)3d\ ^2D_{3/2}$ | 79.34±0.06 | 79.3 [10] | 76.5 [10] | |
| | $3p^5\ ^2P_{1/2}-3p^4(^3P)3d\ ^2P_{1/2}$ | 84.29±0.02 | 84.069 [ 8] | | |
| MoXXVII | $3p^4\ ^3P_2-3p^3(^2P)3d\ ^3P_2$ | 79.74±0.02 | 79.761 [ 8] | | |
| | $3p^4\ ^1D_2-3p^3(^2D)3d\ ^1F_3$ | 80.67±0.06 | 80.403 [ 8] | | |
| | $3p^4\ ^3P_2-3p^3(^2D)3d\ ^3D_3$ | 81.20±0.04 | 81.302 [ 8] | | |
| MoXXVIII | $3p^3\ ^4S_{3/2}-3p^2(^3P)3d\ ^4P_{3/2}$ | 81.87±0.04 | Not observed | | 81.947 [11] |
| | $3p^3\ ^2D_{3/2}-3p^2(^1D)3d\ ^2D_{5/2}$ | 82.54±0.06 | 82.773 [ 8] | | 82.821 [11] |
| | $3p^3\ ^2D_{5/2}-3p^2(^3P)3d\ ^2F_{7/2}$ | 83.21±0.05 | 83.308 [ 7] | | |
| | $3p^3\ ^4S_{3/2}-3p^2(^3P)3d\ ^4P_{5/2}$ | 83.89±0.03 | 83.756 [ 7] | | |
| | $3p^3\ ^2P_{1/2}-3p^2(^1D)3d\ ^2P_{3/2}$ | 84.67±0.05 | 84.771 [ 8] | | |

sitions among $n = 3$ with $\Delta n = 0$. The result of the detailed wavelength identification for Mo lines is presented in Table 1 with their transitions. The numerical values followed $\pm$ sign indicate the accuracy in wavelength measurement. It was estimated from the maximum deviation of weighted peak position of a spectral line in different temporal frames. The theoretically calculated and predicted values are also indicated in the table. The brackets following the values show their references. The calculated values are based on ab initio energy level calculation. The predicted values are based on the extrapolation of experimentally measured energy levels at low-Z elements followed by the ab initio energy level calculation. Only the Mo XXVIII $3p^3$ $^4S_{3/2}$-$3p^2(3P)3d$ $^4P_{3/2}$ transition at $81.947$ Å had not been observed yet, but it has been newly observed in this study, which is presented as $81.87$ Å in the Table 1. As mentioned in table several strong 3p-3d transitions from Mo XXIV to Mo XXVIII are the major contributor of the unresolved spectral array around 65-90 Å.

On the other hand, several other isolated lines are also seen at shorter and longer wavelength sides of the unresolved spectral array in Fig. 1 including several forbidden transitions from Mo XV and Mo XVI [12]. For example two electric quadruple transitions (E2) of $3d^{10}$ $^1S_0$-$3d^9 4s$ $^{1,3}D_2$ in the Ni-like Mo XV can be clearly seen at $57.92$ and $58.83$ Å. The strongest isolated lines are emitted at $115.98$ Å ($3s^2$ $^1S_0$-$3p$ $^1P_1$) and $127.9$ Å ($3s$ $^2S_{1/2}$-$3p$ $^2P_{3/2}$) as a resonance transition of Mg-like Mo XXXI and Na-like Mo XXXII. These charge states exist in the central region of the LHD plasma under the present experimental condition. The intensities of these resonance lines reached to the maximum value after 75 ms of the pellet ablation and frequently saturated in the 16 bit CCD counts. The identification of relatively week spectral lines below 50 Å was not done in the present study because the spectral resolution of the spectrometer rapidly drops at such shorter wavelength range [5]. These spectra likely consist of 3d-4f transitions of Mo XV to Mo XVI and 3d-4p transitions of Mo XVI to Mo XIX [3]. Since these charge states exist in a very narrow radial location near the plasma edge where the electron temperature is relatively low, the molybdenum emissions become weak compare to the other lines from higher charge states.

A molybdenum EUV spectrum in wavelength range of 165-315 Å is shown in Fig.2, which contains several other impurity lines. Such impurity lines are useful for the wavelength calibration. In the figure, then, the spectrum containing several impurity lines was specially selected for good understanding, although the discharge condition was slightly different from the previous one. The 3s-3p doublet ($127.9$ Å, $176.63$ Å, $3s$ $^2S_{1/2}$-$3p$ $^2P_{3/2,1/2}$) in resonance transition of Na-like Mo XXXII are apparent with strong intensities in Figs.1 and 2. A similar type of transition is also seen in Fig.2 from Li-like Fe XXIV at $192.02$ Å ($2s$ $^2S_{1/2}$-$2p$ $^2P_{3/2}$). Other resonance transitions are clearly appeared at $221.15$ Å for Be-like Ar XV ($2s^2$ $^1S_0$-$2s2p$
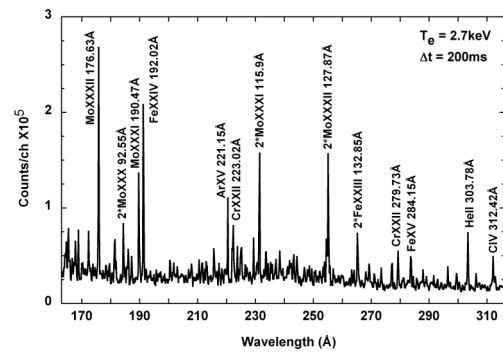


Fig. 2   Mo spectrum in 165-315 Å.
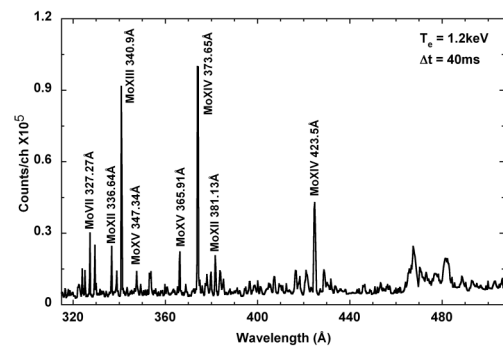


Fig. 3   Mo spectrum in 315-500 Å.

$^1P_1$), $223.02$ and $279.73$ Å for Li-like Cr XXII ($2s$ $^2S_{1/2}$-$2p$ $^2P_{3/2,1/2}$) and $284.15$ Å for Mg-like Fe XV ($3s^2$ $^1S_0$-$3s3p$ $^1P_1$).

Strong resonance lines from lower charge states molybdenum ions of Zn-like Mo XIII ($340.91$ Å, $4s^2$ $^1S_0$-$4s4p$ $^1P_1$) and Cu-like Mo XIV ($373.65$ Å, $423.5$ Å $4s$ $^2S_{1/2}$-$4p$ $^2P_{3/2,1/2}$) are recorded as revealed in Fig. 3. These relatively low ionized states of molybdenum immediately appear after the impurity pellet ablation.

## 3.2   Tungsten

Tungsten lines from different ionization stages in EUV and soft X-ray ranges have been identified with reference to theoretically calculated and experimentally observed values [2, 13–19]. After the carbon pellet containing the tungsten material was injected, the central electron temperature rapidly decreased from 2.2 keV to 0.75 keV due to the ionization and radiation losses and then recovered up to 1.2 keV. Figure 4 shows tungsten spectra in wavelength range of 24-80 Å. The spectrum in Fig. 4 (a) is recorded at $\Delta t = 340$ ms after the injection where the central electron temperature had the lowest value of 0.75 keV. On the contrary the spectrum in Fig. 4 (b) is recorded at $\Delta t = 440$ ms with higher electron temperature of 1.0 keV. Three blended transition bands are visible around 33, 50 and 60 Å.

The band around 33 Å consists of charge states in W XXII-W XXX with ionization potentials of 594.5-

Table 2 Observed transitions of W ions in 24-40 Å.

| Ionization stages | Transitions | Wavelengths (Å) | | | |
|---|---|---|---|---|---|
| | | Present experiment | Previous experiment | Calculated | Predicted |
| WXXII | $4d^{10}4f^7-4d^94f^75p$ | 38.13±0.07 | | 37.57 [18] | |
| | $4f^7-4f^65g$ | | | 37.95 [18] | |
| WXXIII | $4f^6-4f^55g$ | 35.86±0.07 | | 35.93 [18] | |
| | $4d^{10}4f^6-4d^94f^65p$ | | | 36.21 [18] | |
| WXXIV | $4d^{10}4f^5-4d^94f^55p$ | 34.90±0.06 | | 34.85 [18] | |
| | $4f^5-4f^45g$ | 34.12±0.06 | | 34.06 [18] | |
| WXXV | $4f^4-4f^35g$ | 32.50±0.05 | Not measured | 32.43 [18] | |
| WXXVI | $4d^{10}4f^3-4d^94f^35p$ | 32.50±0.05 | | 32.37 [18] | |
| | $4f^3-4f^25g$ | 30.90±0.03 | | 30.94 [18] | |
| WXXIX | $4d^{10}\ ^1S_0-4d^95p\ ^1P_1$ | 29.51±0.03 | | | 29.40 [19] |
| | | 28.32±0.05 | | | |
| | Not identified | 26.87±0.04 | | | |
| | | 25.36±0.05 | | | |
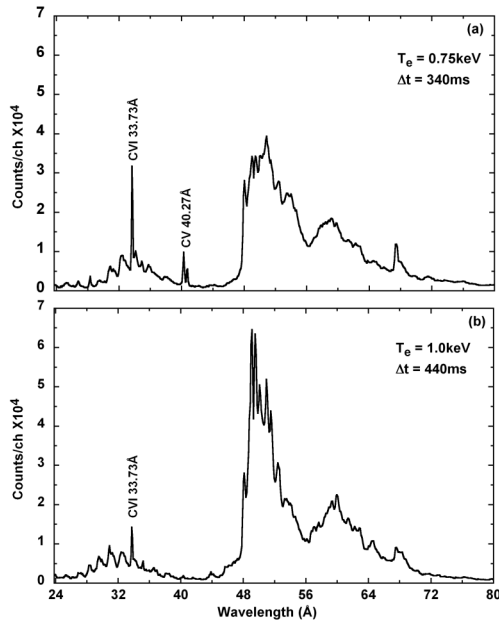


Fig. 4  W spectra in 24-80 Å at (a) $\Delta t$ = 340 ms and (b) $\Delta t$ = 440 ms after pellet injection.

1179.9 eV, respectively. As evidently seen in Fig. 4 the peak position of this band shifts from 34 Å to 31 Å as the electron temperature increases from 0.75 keV to 1.0 keV, whereas the peak positions of the blended band at 50 and 60 Å do not move against such a temperature difference. The spectral lines near 34 Å from low-temperature plasma after 340 ms of the pellet injection peaked at 34 Å are emitted from charge states of W XXII to W XXVI and those near 31 Å from high-temperature plasma after 440 ms are dominated by higher ionization stages, e.g., W XXIX $4d^{10}$ $^1S_0$-$4d^95p$ $^1P_1$, 29.4 Å. Most of these lines have been identified and listed in Table 2. Theoretically calculated values were determined by ab initio calculation on mean wave-

length averaged over large number of transitions using Unresolved Transition Array (UTA) formula. Only the transition of $4d^{10}$ $^1S_0$-$4d^95p$ $^1P_1$ at 29.4 Å was predicted as isoelectronic extrapolation of Pd-like transition observed for lower Z elements. The transitions of W XXII to W XXVI belong to $\Delta n$ = 1 radiative decay with the configurations of $4d^{10}4f^k$-$4d^94f^k5p$ and $4f^k$-$4f^{k-1}5$ g, where $k$ = 3-7. Three observed lines identified as 32.50, 35.86 and 38.13 Å are blended with two transitions as indicated in the Table 2, because of inadequate spectral resolving power of the present spectrometer at such an extremely short wavelength range. The theoretically calculated line at 33.59 Å (W XXV; $4d^{10}4f^4$-$4d^94f^45p$) can not be identified since another strong C VI (33.73 Å) line exists in the same wavelength position.

In the blended bands around 50 and 60 Å several lines are strongly appeared on the top of the pseudo-continuum when the electron temperature recovers up to 1.0 keV as indicated in Fig. 4 (b). The isolated lines observed here are estimated to be from W XXVIII, W XXIX and W XXX, taking into account the ionization potentials and previous works. The transitions identified here are listed in Table 3. Asmussen et al. [2] and J. Sugar et al. [15–17] tabulated many observed, calculated and predicted wavelengths in these band structures and their transitions are also listed in the Table 3 as previous works. The transition at 48.02 Å measured in the present study was originally observed in ORMAK tokamak [13] and considered to be from Au [16], but did not appear in PLT tokamak [14]. It is finally identified here as the tungsten line, since any gold material is not used inside the LHD vacuum chamber. This line is then in good agreement with the predicted wavelength (47.94 Å) of W XXVIII $4d^{10}4f$ $^2F_{5/2}$-$4d^94f^2$ $^2F_{7/2}$ [16]. The emissions around 60 Å are likely to be from triplet transitions of W XXIX $4d^{10}$-$4d^94f$ and W XXVIII $4d^{10}4f$-$4d^94f^2$ [17].

Table 3 Observed transitions of W ions in 50-70 Å.

| Ionization stages | Transitions | Wavelengths (Å) | | | |
|---|---|---|---|---|---|
| | | Present experiment | Previous experiment | Calculated | Predicted |
| WXXVIII | $4d^{10}4f\ ^2F_{7/2}-4d^94f(^1P)4f\ ^2G_{7/2}$ | 52.31±0.03 | 52.35 [13] | | 52.35 [16] |
| | $4d^{10}4f\ ^2F_{5/2}-4d^94f(^1P)4f\ ^2G_{7/2}$ | 51.42±0.02 | 51.457 [16] | 51.245 [16] | 51.455 [16] |
| | $4d^{10}4f\ ^2F_{5/2}-4d^94f(^1P)4f\ ^2G_{9/2}$ | 50.87±0.02 | 50.895 [16] | 50.7 [16] | 50.891 [16] |
| | $4d^{10}4f\ ^2F_{5/2}-4d^94f(^1P)4f\ ^2D_{3/2}$ | 49.44±0.02 | 49.4 [ 2], | 48.919 [16] | 49.405 [16] |
| | $4d^{10}4f\ ^2F_{7/2}-4d^94f(^1P)4f\ ^2D_{5/2}$ | | 49.403 [16] | 48.874 [16] | 49.402 [16] |
| | $4d^{10}4f\ ^2F_{5/2}-4d^94f^2\ ^2F_{7/2}$ | 48.02±0.02 | 47.94 [13] | | 47.94 [16] |
| WXXIX | $4d^{10}\ ^1S_0-4d^94f\ ^3D_1$ | 59.88±0.02 | 59.852 [15] | 59.736 [15] | 59.851 [15] |
| | $4d^{10}\ ^1S_0-4d^94f\ ^1P_0$ | 49.00±0.02 | 48.9 [ 2], 48.948 [15] | 49.295 [15] | 48.944 [15] |
| WXXX | $4d^9\ 2D_{5/2}-4d^8(^1G)4f\ ^2P_{3/2}$ | 49.99±0.03 | 49.938 [17] | 50.034 [17] | 49.936 [17] |
| | | 67.96±0.05 | | | |
| | | 65.87±0.05 | | | |
| | | 64.53±0.04 | | | |
| | | 62.13±0.05 | | | |
| | Not identified | 61.19±0.05 | | | |
| | | 59.17±0.04 | | | |
| | | 57.54±0.03 | | | |
| | | 56.73±0.04 | | | |
| | | 53.32±0.04 | | | |

## 4. Summary

EUV spectra of molybdenum and tungsten have been investigated and several transitions have been newly identified. Carbon pellets containing such materials were injected in LHD for the observation. Molybdenum spectra are observed in 20-500 Å and the pseudo-continuum lines are identified and listed with previous works in wavelength range of 65-90 Å. Some forbidden transitions from Mo XV and Mo XVI are also identified around 55 Å. Although several weak lines are observed below 50 Å, those can not be analyzed due to a poor spectral resolution of the present spectrometer.

Three blended spectral bands are observed for the tungsten spectrum in 24-80 Å. The spectral band at 33 Å shifted to shorter wavelength range when the electron temperature increased from 0.75 keV to 1.0 keV. These spectra are identified as $\Delta n = 1$ transition of W XXII-W XXVI having $4d^{10}4f^k$-$4d^94f^k5p$ and $4d^{10}4f^k$-$4d^94f^{k-1}5g$, where $k = 3$-$7$. Isolated lines were seen on the top of the pseudo-continuum in 50-70 Å when the electron temperature increased up to 1.0 keV. Those are identified as $\Delta n = 0$ transitions of W XXVIII-W XXX. These tungsten lines observed here are also listed in the table with previous works. In the future a detail analysis on EUV spectra will be stud-

ied below 50 Å using an EUV spectrometer with better resolution.

[1]  G. Federici *et al.*, Nucl. Fusion **71**, 1967 (2001).
[2]  K. Asmussen *et al.*, Nucl. Fusion **38**, 967 (1998).
[3]  M. J. May *et al.*, Nucl. Fusion **37**, 881 (1997).
[4]  H. Nozato, S. Morita, M. Goto *et al.*, Rev. Sci. Instrum. **74**, 2032 (2003).
[5]  M.B. Chowdhuri, S. Morita, M. Goto *et al.*, Rev. Sci. Instrum. **78**, 023501 (2007).
[6]  R. Katai, S. Morita, M. Goto *et al.*, *to be published in* Jpn. J. Appl. Phys.
[7]  NIST online Atomic data base; http://physics.nist.gov/ PhysRefData/ASD/index.html.
[8]  C. Jupen *et al.*, Phys. Scr. **68**, 230 (2003).
[9]  A. Wouters *et al.*, J. Opt. Soc. Am. B **5**, 1520 (1988).
[10]  M. Finkenthal *et al.*, J. Phys. B: At. Mol. Phys. **18**, 4393 (1985).
[11]  J. Sugar *et al.*, J. Opt. Soc. Am. B **8**, 22 (1991).
[12]  J. Sugar *et al.*, Phys. Rev. A **51**, 835 (1995).
[13]  R.C. Isler *et al.*, Phys. Lett. **63A**, 295 (1977).
[14]  E. Hinnov and M. Mittaioli, Phys. Lett. **66A**, 109 (1978).
[15]  J. Sugar *et al.*, J. Opt. Soc. Am. B **10**, 799 (1993).
[16]  J. Sugar *et al.*, J. Opt. Soc. Am. B **10**, 1321, (1993).
[17]  J. Sugar *et al.*, J. Opt. Soc. Am. B **10**, 1977 (1993).
[18]  M. Finkenthal *et al.*, Phys. Lett. A **127**, 255 (1988).
[19]  J. Sugar and V. Kaufman PRA **21**, 2096 (1980).